Information Sciences Letters
An International Journal

http://dx.doi.org/10.18576/isl/050102

Combined Effects of Variable Thermal Conductivity and MHD Flow on Pseudoplastic Fluid over a Stretching Cylinder by using Keller Box Method

T. Salahuddin[*], *M. Y. Malik, Arif Hussain, S. Bilal and M. Awais.*

Department of Mathematics, Quaid-i-Azam University Islamabad, 44000, Pakistan.

Received: 7 Jun. 2015, Revised: 21 Sep. 2015, Accepted: 23 Sep. 2015
Published online: 1 Jan. 2016

Abstract: This analysis deals with the numerical solution of MHD flow of tangent hyperbolic fluid over a stretching cylinder in the presence of variable thermal conductivity. The governing nonlinear partial differential equations are presented and then converted into ordinary differential equations by using similarity transformations. The subsequent ordinary differential equations are successfully solved by using implicit finite difference scheme known as the Keller-box method. The non-dimensional parameters appearing in momentum and temperature equations are expressed through graphs in order to analyze the behavior of velocity and temperature profiles. To understand the behavior of fluid near the surface of the cylinder the skin friction co-efficient and local heat flux are calculated graphically and in tabulated form.

Keywords: Variable thermal conductivity; Tangent hyperbolic fluid; MHD flow; Stretching cylinder; Keller box method.

1 Introduction

The thermo-physical properties such as variable thermal conductivity of the ambient fluid may vary with temperature. The constant thermal conductivity of the fluid condenses the mathematical difficulty of the temperature equation and the analytical solution can be achieved easily [1]. However, the nonlinearity in temperature equation increases by taking the conductivity of the fluid to be variable. Therefore, its analytical solution is not possible. There are so many numerical techniques available to solve these types of equations. Rahman et al. [2] studied the natural convective hydromagnetic flow with variable thermal conductivity and viscosity of micropolar fluid over an inclined permeable plate and solved the problem by using shooting method. They found that for both electrically and non-conducting fluids the shear stress rises with the increase in thermal conductivity parameters. Prasad et al. [3] used Keller box method to solve the hydromagnetic flow of viscous fluid with variable properties over a non-linear stretching sheet. They examined that boundary layer thickness decreases by increasing the Prandtl number. Rangi et al. [4] deliberated the heat transfer of viscous fluid over a stretching cylinder with variable thermal conductivity and solved the equations by using Keller box method. They analyzed that heat transfer increases by increasing curvature of the cylinder. Abel et al. [5] discussed the MHD flow of power law fluid model over a vertical stretching sheet by taking the effects of variable thermal conductivity and thermal buoyancy. They initiated that temperature of the fluid increases by increasing variable thermal conductivity parameter in the prescribed surface temperature condition and decreases in the prescribed surface heat flux condition. Sun et al. [6] investigated the convective-radiative transfer of a moving rod with variable thermal conductivity by using spectral collocation method. They compared the analytical solution with spectral collocation method and concluded that the results are approximately equal.

The magnetic field is valuable in the manufacturing to control the rate of cooling involved in these processes. Some of the practical examples of magnetic field are electronic packages, pumps, thermal insulators, MHD flow meters, MHD power generation, fusing of metals in an electrical furnace etc. Turkyilmazoglu [7] explored the MHD flow of viscoelastic fluid over a stretching sheet by taking the slip effects. He found that by increasing

[*] Corresponding author e-mail: taimoor_salahuddin@yahoo.com

magnetic field the heat transfer rate decreases in the absence of slip condition's, but for non-zero slip the heat transfer rate decreases by increasing magnetic field at the first branch, while a small rise takes place in the second branch. Nadeem et al. [8] inspected the Casson fluid model over a shrinking sheet by applying taking MHD effects. They solved the problem by using adomian decomposition method and found that by increasing the Casson fluid parameter the boundary layer thickness and velocity profile decreases. Akbar et al. [9] presented the MHD flow of Eyring-Powell fluid over a stretching sheet and solved the problem by using implicit difference method with quasi-linearization technique. They analyzed that due to magnetic field and Eyring-Powell fluid parameter the resistance to flow increases so the velocity decreases. Nadeem et al. [10] conducted a study on obliquely striking rheological fluid over a stretching sheet by taking the combined effects of partial slip and magnetic field. They suggested that by increasing slip parameter and magnetic field both tangential and normal velocity decreases.

The pseudoplastic fluids are such fluids which describe the shear thinning effects. Examples of such fluids are blood, paint, nail polish etc. Tangent hyperbolic fluid is one of those fluids. Nadeem et al. [11] studied the peristaltic flow of tangent hyperbolic fluid in a curved channel. They found that by increasing the curvature parameter the size of the bolus decreases in the lower half of channel while remains invariant on the upper half of the channel. Akbar et al. [12] presented the MHD flow of tangent hyperbolic fluid towards a stretching sheet. They observed that thickness of the fluid increases by increasing Weissenberg number and the skin friction increases by increasing power law index and Weissenberg number. Naseer et al. [13] analyzed the tangent hyperbolic fluid over a vertical exponentially stretching cylinder and used Runge-Kutta-Fehlberg method to find its solution. The objective of the present work is to discuss the variable thermal conductivity of MHD tangent hyperbolic fluid over a linearly stretching cylinder. In section II mathematical formulation of the tangent hyperbolic fluid is presented. The Keller box method and its convergence criteria are discussed in section III. In section IV results and discussion of the problem are elaborated. Finally conclusions are shortened in section V.

2 Mathematical Formulation

Consider a steady, two-dimensional boundary layer flow of tangent hyperbolic fluid over a stretching cylinder. The flow is being limited to $r > 0$. The stretching velocity is assumed to be of the form $u = \frac{ax}{l}$ where a is positive constant and l is characteristic length. A unifrom transverse magnetic field B_0 is applied normal to the cylinder. The temperature of the wall is T_p while the ambient temperature of the fluid is T_∞ as shown in **Fig. 1**.

After applying the boundary layer approximation the momentum and energy equations take the form:

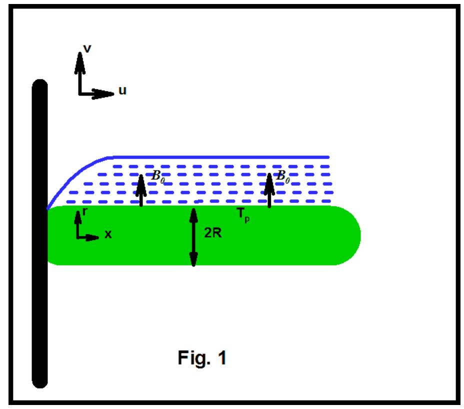

Fig. 1: Geometry of the problem

$$\frac{\partial (ru)}{\partial x} + \frac{\partial (rv)}{\partial r} = 0, \tag{1}$$

$$u\frac{\partial u}{\partial x} + v\frac{\partial u}{\partial r} = \nu\Big((1-n)\frac{\partial^2 u}{\partial r^2} + (1-n)\frac{1}{r}\frac{\partial u}{\partial r} + n\sqrt{2}\Gamma\frac{\partial u}{\partial r}\frac{\partial^2 u}{\partial r^2} + \frac{n\Gamma}{\sqrt{2}r}\Big(\frac{\partial u}{\partial r}\Big)^2\Big) - \frac{\sigma B_0^2}{\rho}u, \tag{2}$$

$$u\frac{\partial T}{\partial x} + v\frac{\partial T}{\partial r} = \frac{1}{r}\frac{\partial}{\partial r}\left(k^* r\frac{\partial T}{\partial r}\right), \tag{3}$$

where $k^* = k(1+\varepsilon\theta)$.
The corresponding boundary conditions are

$$\begin{aligned} &u = U_w(x) = \frac{ax}{l}, \quad v = 0, \\ &T = T_p \text{ at } r = R, \\ &u \to U_\infty(x) = 0,\ T \to T_\infty \text{ as } r \to \infty. \end{aligned} \tag{4}$$

Where k is the constant conductivity of the fluid, Γ is the Williamson parameter, ρ is the density, ν is the kinematic viscosity, σ is the electric charge density, u and v are the velocity components along x and r- axes, respectively. n is the power law index, B_0 is the magnitude of magnetic field, U_w is the stretching velocity, U_∞ is the free stream velocity.

The similarity transformations are:

$$\begin{aligned} \eta &= \sqrt{\frac{a}{l\nu}}\left(\frac{r^2-R^2}{2R}\right), \ \psi = \sqrt{\frac{\nu a x}{l}}Rf(\eta) \\ u &= \frac{1}{r}\frac{\partial \psi}{\partial r}, \ v = -\frac{1}{r}\frac{\partial \psi}{\partial x}, \\ \theta(\eta) &= \frac{T-T_\infty}{T_p-T_\infty}. \end{aligned} \tag{5}$$

The momentum and the temperature equations takes the form:

$$(1-n)(1+2K\eta)f'''+ff''-(f')^2 +2K(1-n)f''+2\lambda n(1+2K\eta)^{\frac{3}{2}}f''f''' +3\lambda K(1+2K\eta)^{\frac{1}{2}}(f'')^2-M^2f'=0, \quad (6)$$

$$(1+2K\eta)(1+\varepsilon\theta)\theta''+2K(1+\varepsilon\theta)\theta' +(1+2K\eta)\varepsilon(\theta')^2+Pr\theta' f=0, \quad (7)$$

the transformed boundary conditions are

$$f(0)=0,\ f'(0)=1,\ \theta(0)=1,\quad f'(\infty)=0,\ \theta(\infty)=0. \quad (8)$$

Where $Pr=\frac{v}{k}$ is the Prandtl number, $K=\frac{1}{R}\sqrt{\frac{vl}{a}}$ denotes the curvature parameter, ε is the thermal conductivity parameter, $\lambda=\frac{\Gamma a^{3/2}x}{\sqrt{2vl^{\frac{3}{2}}}}$ is the dimensionless Weissenberg number and $M^2=\frac{\sigma B_0^2 l}{\rho a}$ is the Hartmann number.

The physical quantities such as coefficient of skin friction and local nusselt number are defined as

$$C_f=\frac{\tau_w}{\frac{\rho a^2x^2}{2l^2}},\ Nu_x=\frac{xq_w}{k(T_p-T_\infty)}, \quad (9)$$

where

$$\tau_w=\mu\left((1-n)\frac{\partial u}{\partial r}+\frac{n}{\sqrt{2}}\Gamma(\frac{\partial u}{\partial r})^2\right)_{r=R},\quad q_w=-k\left(\frac{\partial T}{\partial r}\right)_{r=R}, \quad (10)$$

In dimensionless form the skin friction and local nusselt number are

$$C_fRe_x^{1/2}=(1-n)f''(0)+n\lambda f''^2(0),\quad Nu_xRe_x^{-1/2}=-\theta'(0). \quad (11)$$

Where $Re_x^{1/2}=\frac{a^{1/2}x}{v^{1/2}l^{1/2}}$.

3 Numerical Solutions

By using Keller box $Eq.(6)$ and (7) subject to boundary conditions (8) requires four steps to solve:

1. Equations should be reduced into first-order system.
2. By using central difference approximation write the difference equations.
3. The non-linear algebraic equations should be linearized and write them in matrix-vector form.
4. The linear system should be solved by using block-tridiagonal-elimination method.

3.1 First-Order System

Let u, v, w, g and t be new dependent variables can written in the form

$$u=f', \quad (12)$$

$$v=u', \quad (13)$$

$$t=\theta', \quad (14)$$

after putting all these expressions in $Eq.(6)$ and (7) takes the form

$$(1-n)(1+2K\eta)v'+2(1-n)Kv+3n\lambda (1+2K\eta)^{1/2}Kv^2+2n\lambda(1+2K\eta)^{3/2}vw +fv-u^2-M^2u=0, \quad (15)$$

$$(1+\varepsilon g)(1+2K\eta)t'+2K(1+\varepsilon g)t+(1+2K\eta)\varepsilon t^2 +\mathrm{Pr}tf=0 \quad (16)$$

3.2 Difference Formulation:

Let us consider a net rectangle in $x-\eta$ plane as shown in **Figure 2** and the net points are:

$$x^0=0,\ x^i=x^{i-1}+k_i,\quad i=1,2,3...I,$$
$$\eta_0=0,\ x^i=\eta_{j-1}+h_j,\quad j=1,2,3...J,$$

where k_i is the Δx-spacing and h_j is the $\Delta\eta$-spacing.

Fig. 2. Difference Approximation.

The algebraic form of $Eq.(12)-(14)$ at midpoint $(x^i,\eta_{j-1/2})$ by using centered difference derivatives are

$$\frac{f_j^i-f_{j-1}^i}{h_j}=\frac{u_j^i+u_{j-1}^i}{2}, \quad (17)$$

$$\frac{u_j^i-u_{j-1}^i}{h_j}=\frac{v_j^i+v_{j-1}^i}{2}, \quad (18)$$

$$\frac{\theta_j^i-\theta_{j-1}^i}{h_j}=\frac{t_j^i+t_{j-1}^i}{2}. \quad (19)$$

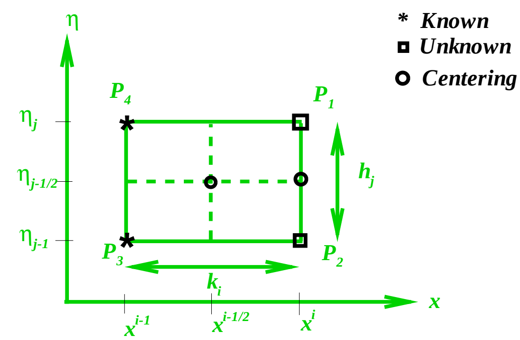

Fig. 2: Difference Approximation

Now, at mid-point $(x^{i-1/2}, \eta_{j-1/2})$ the first order differential $Eq.(15)$ and (16) are approximated

$$\begin{aligned}(1-n)(1+2K\eta)(v_j^i - v_{j-1}^i) + 2(1-n)Khv_{j-1/2}^i \\ +3\lambda n(1+2K\eta)^{1/2}kh(v_{j-1/2}^i)^2 + 2n\lambda h(1+2K\eta)^{3/2} \\ v_{j-1/2}^i w_{j-1/2}^i + h(u_{j-1/2}^i)^2 + f_{j-1/2}^i v_{j-1/2}^i \\ -M^2 u_{j-1/2}^i = Q_{j-1/2},\end{aligned} \tag{20}$$

$$\begin{aligned}(1+2K\eta)(t_j^i - t_{j-1}^i) + 2Kh(1+\varepsilon g_{j-1/2}^i)t_{j-1/2}^i \\ +(1+2K\eta)h\varepsilon(t_{j-1/2}^i)^2 + \Pr ht_{j-1/2}^i t_{j-1/2}^i \\ = N_{j-1/2},\end{aligned} \tag{21}$$

where

$$\begin{aligned}Q_{j-1/2} = -((1-n)(1+2K\eta)(v_j^{i-1} - v_{j-1}^{i-1}) \\ +2(1-n)Khv_{j-1/2}^{i-1} + 3\lambda n(1+2K\eta)^{1/2} \\ khv_{j-1/2}^{i-1} + 2n\lambda h(1+2K\eta)^{3/2} v_{j-1/2}^{i-1} w_{j-1/2}^{i-1} \\ +h(u_{j-1/2}^{i-1})^2 + f_{j-1/2}^{i-1} v_{j-1/2}^{i-1} - M^2 u_{j-1/2}^{i-1}),\end{aligned}$$

and

$$\begin{aligned}N_{j-1/2} = -((1+2K\eta)(t_j^{i-1} - t_{j-1}^{i-1}) \\ +2Kh(1+\varepsilon g_{j-1/2}^{i-1})t_{j-1/2}^{i-1} + (1+2K\eta)h\varepsilon \\ (t_{j-1/2}^{i-1})^2 + \Pr ht_{j-1/2}^{i-1} t_{j-1/2}^{i-1}).\end{aligned}$$

Where $Q_{j-1/2}$ and $N_{j-1/2}$ are the known quantities. The boundary conditions can be writen in the form

$$\begin{aligned}f_0^i = 0,\ u_0^i = 1,\ u_J^i = 0, \\ g_0^i = 1,\ g_J^i = 0.\end{aligned} \tag{22}$$

3.3 Newton's Method

The $Eqs.(17) - (21)$ can be linearized by using Newton's method. For this case

$$\begin{aligned} f_j^{(i+1)} &= f_j^{(i)} + \delta f_j^{(i)}, \\ u_j^{(i+1)} &= u_j^{(i)} + \delta u_j^{(i)}, \\ v_j^{(i+1)} &= v_j^{(i)} + \delta v_j^{(i)}, \\ g_j^{(i+1)} &= g_j^{(i)} + \delta g_j^{(i)}, \\ t_j^{(i+1)} &= t_j^{(i)} + \delta t_j^{(i)}, \end{aligned} \tag{1}$$

putting these terms in $Eqs.(17) - (21)$ and neglecting the higher order of δ

$$\delta f_j - \delta f_{j-1} - \frac{h_j}{2}(\delta u_j + \delta u_{j-1}) = (r_1)_j, \tag{24}$$

$$\delta u_j - \delta u_{j-1} - \frac{h_j}{2}(\delta v_j + \delta v_{j-1}) = (r_2)_j, \tag{25}$$

$$\delta \theta_j - \delta \theta_{j-1} - \frac{h_j}{2}(\delta t_j + \delta t_{j-1}) = (r_3)_j, \tag{26}$$

$$\begin{aligned}(a_1)_{j-1/2}\delta v_j + (a_2)_{j-1/2}\delta v_{j-1} + (a_3)_{j-1/2}\delta u_j \\ +(a_4)_{j-1/2}\delta u_{j-1} + (a_5)_{j-1/2}\delta f_j \\ +(a_6)_{j-1/2}\delta f_{j-1} = (r_4)_{j-1/2},\end{aligned} \tag{27}$$

$$\begin{aligned}(b_1)_{j-1/2}\delta t_j + (b_2)_{j-1/2}\delta t_{j-1} + (b_3)_{j-1/2}\delta g_j \\ +(b_4)_{j-1/2}\delta g_{j-1} + (b_5)_{j-1/2}\delta f_j \\ +(b_6)_{j-1/2}\delta f_{j-1} = (r_5)_{j-1/2},\end{aligned} \tag{2}$$

where

$$\begin{aligned}(a_1)_{j-1/2} = (1-n)(1+2K\eta) + (1-n)Kh \\ +3\lambda n(1+2K\eta)^{1/2}khv_{j-1/2} + 2n\lambda \\ (1+2K\eta)^{3/2}v_{j-1/2} + n\lambda h(1+2K\eta)^{3/2}w_{j-1/2} \\ +\frac{hf_{j-1/2}}{2},\end{aligned} \tag{29}$$

$$(a_2)_{j-1/2} = -(1-n)(1+2K\eta)+(1-n)Kh \\ +3\lambda n(1+2K\eta)^{1/2}khv_{j-1/2}-2n\lambda \\ (1+2K\eta)^{3/2}v_{j-1/2}+n\lambda h(1+2K\eta)^{3/2}w_{j-1/2} \\ +\frac{hf_{j-1/2}}{2}, \quad (30)$$

$$(a_3)_{j-1/2} = -hu_{j-1/2}-\frac{hM^2}{2}, \\ (a_4)_{j-1/2} = (a_3)_{j-1/2}, \quad (31)$$

$$(a_5)_{j-1/2} = \frac{hv_{j-1/2}}{2}, \\ (a_6)_{j-1/2} = (a_5)_{j-1/2}, \quad (32)$$

$$(b_1)_{j-1/2} = (1+2K\eta)(1+\varepsilon g_{j-1/2})-\frac{\varepsilon g_{j-1/2}}{2} \\ +2Kh+Kh\varepsilon g_{j-1/2}+(1+2K\eta)h\varepsilon t_{j-1/2} \\ +\frac{\Pr hf_{j-1/2}}{2}, \quad (33)$$

$$(b_2)_{j-1/2} = (1+2K\eta)(-1-\frac{\varepsilon g_{j-1/2}}{2})+Kh\varepsilon g_{j-1/2} \\ +2Kh+(1+2K\eta)h\varepsilon t_{j-1/2}+\frac{\Pr hf_{j-1/2}}{2}, \\ (34)$$

$$(b_3)_{j-1/2} = (1+2K\eta)(\frac{t_j}{2}-\frac{\varepsilon t_{j-1}}{2})+\frac{\varepsilon t_{j-1}}{2}, \\ (b_4)_{j-1/2} = (b_3)_{j-1/2} \quad (35)$$

$$(b_5)_{j-1/2} = \frac{\Pr ht_{j-1/2}}{2}, \\ (b_6)_{j-1/2} = (b_5)_{j-1/2}, \quad (36)$$

$$(r_4)_{j-1/2} = -h(1-n)(1+2K\eta)w_{j-1/2} \\ -2(1-n)Khv_{j-1/2}-3\lambda n(1+2K\eta)^{1/2}kh(v_{j-1/2})^2 \\ -2n\lambda h(1+2K\eta)^{3/2}v_{j-1/2}w_{j-1/2}-hf_{j-1/2}v_{j-1/2} \\ -h(u_{j-1/2})^2+M^2u_{j-1/2}+Q_{j-1/2}, \\ (37)$$

$$(r_5)_{j-1/2} = -(1+2K\eta)t_j-\varepsilon t_j g_{j-1/2} \\ +(1+2K\eta)t_{j-1}+(1+2K\eta)\varepsilon t_{j-1}g_{j-1/2} \\ -2Kh(t_{j-1/2}+\varepsilon t_{j-1/2}g_{j-1/2})-(1+2K\eta) \\ h\varepsilon t_{j-1/2}-\Pr ht_{j-1/2}f_{j-1/2}+N_{j-1/2}, \quad (38)$$

after applying the Newton's method the boundary conditions become:

$$\delta f_0 = 0,\ \delta u_0 = 0,\ \delta t_0 = 0, \\ \delta u_J = 0,\ \delta t_J = 0. \quad (39)$$

3.4 The Block Tridiagonal structure:

The linearized system of equations takes the block tridiagonal form. i.e

$$[A][\delta] = [r], \quad (40)$$

$$\begin{bmatrix} [A_1] & [C_1] & & & & \\ [B_1] & [A_2] & [C_2] & & & \\ & - & - & - & & \\ & & - & - & - & \\ & & & - & - & - \\ & & & [B_{J-1}] & [A_{J-1}] & [C_{J-1}] \\ & & & & [B_J] & [A_J] \end{bmatrix} \begin{bmatrix} [\delta_1] \\ [\delta_2] \\ - \\ - \\ - \\ [\delta_{J-1}] \\ [\delta_J] \end{bmatrix} = \begin{bmatrix} [r_1] \\ [r_2] \\ - \\ - \\ - \\ [r_{J-1}] \\ [r_J] \end{bmatrix}$$

where the elements are defined as: where $d = \frac{-h_j}{2}$.

By using **LU method** this block tridiagonal matrix given in $Eq.(40)$ is solved. From this block tridiagonal matrix the solution of $[\delta]$ is calculated and these calculations are repeated until some convergence criterion is satisfied and is stopped when

$$|\delta v_0^{(i)}| \leq \varkappa \quad (41)$$

where $\varkappa = 0.001$ is a small value.

4 Results and Discussion

In this section the physical interpretation of different parameters appearing in momentum and temperature

$$[A_1] = \begin{bmatrix} 0 & 0 & 1 & 0 & 0 \\ d & 0 & 0 & d & 0 \\ 0 & d & 0 & 0 & d \\ a_2 & 0 & a_5 & a_1 & 0 \\ 0 & b_2 & b_5 & 0 & b_1 \end{bmatrix}$$

$$[C_j] = \begin{bmatrix} d & 0 & 0 & 0 & 0 \\ 1 & 0 & 0 & d & 0 \\ 0 & 1 & 0 & 0 & d \\ a_3 & 0 & 0 & 0 & 0 \\ 0 & b_3 & 0 & 0 & 0 \end{bmatrix}$$

$$[A_j] = \begin{bmatrix} d & 0 & 1 & 0 & 0 \\ -1 & 0 & 0 & d & 0 \\ 0 & -1 & 0 & 0 & d \\ a_4 & 0 & a_5 & a_1 & 0 \\ 0 & b_4 & b_5 & 0 & b_1 \end{bmatrix}$$

$$[B_j] = \begin{bmatrix} 0 & 0 & -1 & 0 & 0 \\ 0 & 0 & 0 & d & 0 \\ 0 & 0 & 0 & 0 & d \\ 0 & 0 & a_6 & a_2 & 0 \\ 0 & 0 & b_6 & 0 & b_2 \end{bmatrix}$$

equations are deliberated. **Fig. 3a** shows the effect of Weissenberg number λ on velocity profile. As the Weissenberg number λ increases the relaxation time of the fluid increases, causing the viscosity of the fluid to increases. As a result velocity of the fluid reduces. **Fig. 3b** illustrates the behavior of curvature parameter K on velocity profile. As the curvature of the cylinder is increased, the radius of cylinder reduces. As a consequence, area of the cylinder decreases. Hence less resistance is offered by cylinder to the fluid particles so velocity enhances. **Fig. 3c** shows effect of Hartmann number M on velocity profile. As Hartmann number M grows the Lorentz forces rises which produce resistance to flow, causing velocity of the fluid to reduce. **Fig. 3d** depicts the effect of power law index n on velocity profile. The effect of increasing power law index n is to decelerate the boundary layer thickness. The temperature profile revealed in **Fig. 3e** display that as the Prandtl number Pr increases the thermal boundary layer thickness decelerates. **Fig. 3f** shows the behavior of variable thermal conductivity parameter ε on temperature profile. It is observed that the kinetic energy of fluid particles enriches by increasing variable thermal conductivity parameter ε which causes increase in the thermal boundary layer thickness and the temperature profile. The impact of Hartmann number M and power law index n on skin friction coefficient are presented in **Fig. 4a** and **b** versus Weissenberg number λ. From **Fig. 4a** it is immersed that resistance to flow rises with the increase in Hartmann number M but opposite behavior is shown in the case of Weissenberg number λ. On the other hand, resistance to flow decreases the skin friction with the increase in power law index n as shown in **Fig. 4b**. **Fig. 4c** shows the effect Prandtl number Pr on Nusselt number versus variable thermal conductivity parameter ε. It is observed from the figure that Nusselt number increases by increasing Prandtl number Pr but variable thermal conductivity causes decrease in Nusselt number. Because by increasing variable thermal conductivity the viscosity of the fluid decreases so magnitude of rate of convectional heat transfer also decreases.

5 Concluding Remarks

Variable thermal conductivity in two dimensional MHD flow of tangent hyperbolic fluid is examined over a linear stretching cylinder. An efficient technique Keller box method is utilized to calculate the solution of the ordinary

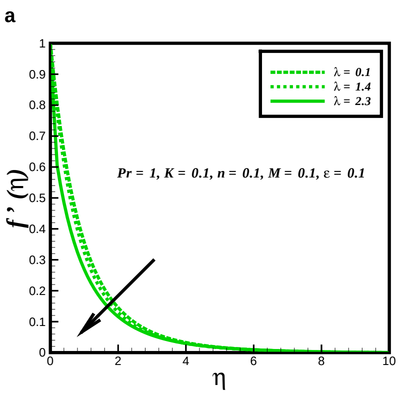

Fig. 3a Influence of λ on $f'(\eta)$

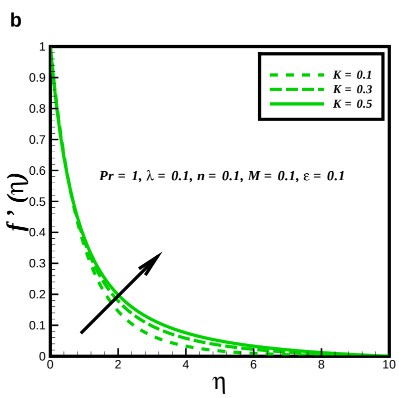

Fig. 3b Influence of K on $f'(\eta)$

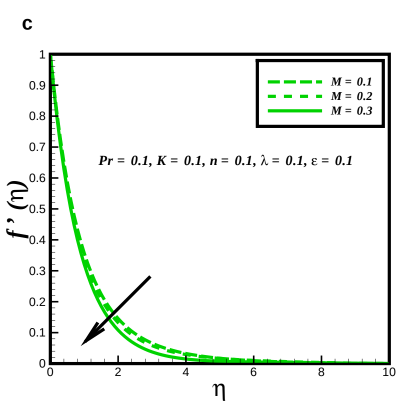

Fig. 3c Influence of M on $f'(\eta)$

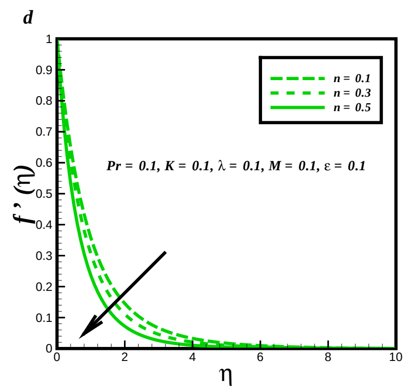

Fig. 3d Influence of n on $f'(\eta)$

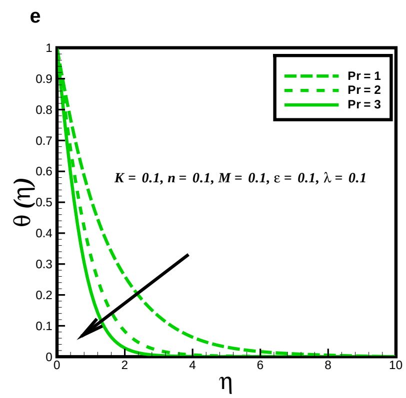

Fig. 3e Influence of Pr on $\theta(\eta)$

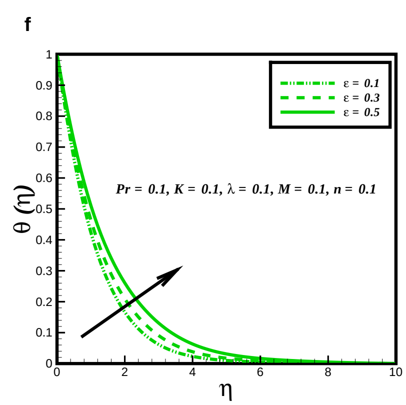

Fig. 3f Influence of ε on $\theta(\eta)$

differential equations. The dimensionless parameters involve in the equations are examined through tables and graphs. It is observed that velocity of the fluid decreases by increasing Weissenberg number λ, Hartmann number M and power law index n. While by varying variable thermal conductivity parameter ε the temperature of the fluid rises but it decreases by increasing Prandtl number Pr. The skin friction shows dominant effect in the case of

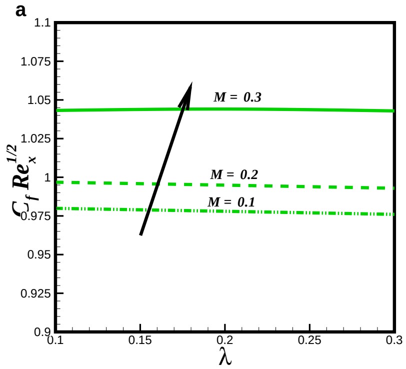

Fig. 4a Influence of M and λ on skin friction

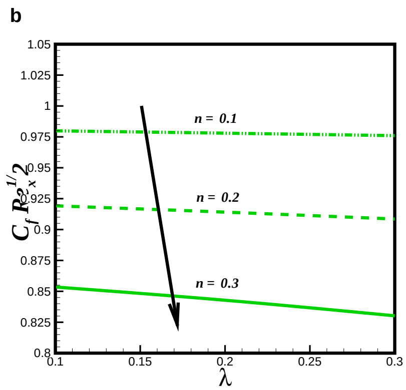

Fig. 4b Influence of n and λ on skin friction

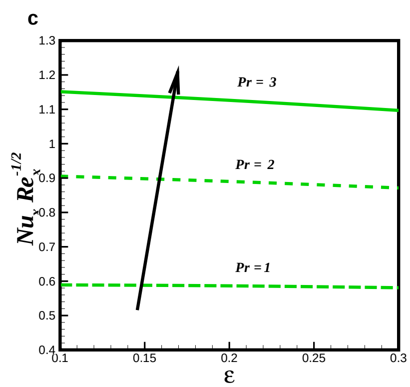

Fig. 4c Influence of ε and Pr on Nusselt number

Hartmann number M and power law index n but shows decreasing behavior by increasing Weissenberg number λ. The heat transfer rate rises by increasing Prandtl number Pr but it decreases by increasing variable thermal conductivity parameter ε.

Table 1: Numerical values of $C_f Re_x^{1/2}$ for K, λ, n and M.

K	λ	n	M	$C_f Re_x^{1/2}$
0.1	0.1	0.1	0.1	-0.9799
0.2				-1.0098
0.3				-1.0393
0.1	0.1			-0.9799
	0.2			-0.9780
	0.3			-0.9760
	0.1	0.1		-0.9799
		0.2		-0.9192
		0.3		-0.8535
		0.1	0.1	-0.9799
			0.2	-0.9968
			0.3	-1.0432

Table 2: Numerical values of $Nu_x Re_x^{-1/2}$ for K, Pr and ε.

K	Pr	ϵ	$Nu_x Re_x^{-1/2}$
0.1	1	0.1	0.6321
0.2			0.5959
0.3			0.5744
0.1	1		0.6321
	2		0.8624
	3		1.0767
	1	0.1	0.6321
		0.2	0.6112
		0.3	0.5921

References

[1] A.D. Kraus, A. Aziz, J.R. Welty, Extanded surface heat transfer, Wiley, New York, 2011.

[2] M.M. Rahman, A. Aziz, M.A. Al-Lawatia, Heat transfer in micropolar fluid along an inclined permeable plate with variable fluid properties, Internationl Journal of thermal sciences,49 (2010)93-1002.

[3] K.V. Prasad, K. Vajravelu, P.S. Datti, The effects of variable fluid properties on the hydro-magnetic flow and heat transfer over a non-linearly stretching sheet, International Journal of Thermal Sciences, 49 (2010) 603–610.

[4] R.R. Rangi, N. Ahmad, Boundary Layer Flow past a Stretching Cylinder and Heat Transfer with Variable

Thermal Conductivity, Applied Mathematics, 3 (2012) 205-209.

[5] M.S. Abela, P.G. Siddheshwar, N. Mahesha, Effects of thermal buoyancy and variable thermal conductivity on the MHD flow and heat transfer in a power-law fluid past a vertical stretching sheet in the presence of anon-uniform heat source, International Journal of Non-Linear Mechanics, 44 (2009) 1–12.

[6] Ya. Song Sun, Jing Ma, Ben-Wen Li, Spectral collocation method for convective-radiative transfer of a moving rod with variable thermal conductivity, International journal of thermal science, 90 (2015) 187-196.

[7] M. Turkyilmazoglu, Multiple solutions of heat and mass transfer of MHD slip flow for the viscoelastic fluid over a stretching sheet, Internationl Journal of thermal sciences, 50 (2011)2264-2276.

[8] S. Nadeem, Rizwan Ul Haq, C. Lee, MHD flow of a Casson fluid over an exponentially shrinking sheet, Scientia Iranica B 19 (2012) 1550–1553.

[9] N.S. Akbar, A. Ebaid, Z.H. Khan, Numerical analysis of magnetic field effects on Eyring-pPowell fluid flow towards a stretching sheet, Journal of Magnetism and Magnetic Materials, 382 (2015) 355-358.

[10] S. Nadeem, R. Mehmood, N.S. Akbar, Combined effects of magnetic field and partial slip on obliquely striking rheological fluid over a stretching surface, Journal of Magnetism and Magnetic Materials, 378 (2015) 457-462.

[11] S. Nadeem, E.N. Maraj, The mathematical analysis for peristaltic flow of hyperbolic tangent fluid in a curved channel, Communications in Theoretical Physics, 59 (2013) 729-736.

[12] N.S. Akbar,S. Nadeem, R.U. Haq, Z.H. Khan, Numerical solutions of Magnetohydrodynamic boundaey layer flow of tangent hyperbolic fluid towards a stretching sheet, Indian Journal of Physics, 87 (2013) 1121-1124.

[13] M. Naseer, M.Y. Malik, S. Nadeem, A. Rehman, The boundary layer flow of hyperbolic tangent fluid over a vertical exponentially stretching cylinder, Alexandria Engineering Journal, 53(2014) 747–750.

T. Salahuddin is working as a PhD Scholar in the department of Mathematics at Quaid-i-Azam University, Islamabad under the supervision of Dr. M.Y. Malik. He obtained his MS degree with distinction and published his research articles in internationally refereed journals. His studies are focused on analysis of computational fluid dynamics.

M. Y. Malik is Professor at Quaid-i-Azam University Islamabad. He has published many papers in the area of computational fluid dynamics. His has 15 years' experience in research.

Arif Hussain is working as a PhD Scholar in the department of Mathematics at Quaid-i-Azam University, Islamabad under the supervision of Dr. M.Y. Malik. He obtained his MS degree with distinction and published his research articles in internationally refereed journals. His studies are focused on analysis of computational fluid dynamics.

S. Bilal is working as a PhD Scholar in the department of Mathematics at Quaid-i-Azam University, Islamabad under the supervision of Dr. M.Y. Malik. He obtained his MS degree with distinction and published his research articles in internationally refereed journals. His studies are focused on analysis of computational fluid dynamics.

M. Awais is working as a PhD Scholar in the department of Mathematics at Quaid-i-Azam University, Islamabad under the supervision of Dr. M.Y. Malik. He obtained his MS degree with distinction and published his research articles in internationally refereed journals. His studies are focused on analysis of computational fluid dynamics.